Resource recovery from digested manure centrate: Comparison between conventional and aquaporin thin-film composite forward osmosis membranes

Revised manuscript submitted to *Journal of Membrane Science*

August 2019

Yun Li [a], Zhicheng Xu [a], Ming Xie [b], Bangxi Zhang [c], Guoxue Li [a], Wenhai Luo [a, d*]

[a] *Beijing Key Laboratory of Farmland Soil Pollution Prevention and Remediation, College of Resources and Environmental Sciences, China Agricultural University, Beijing, 100193, China*

[b] *Department of Chemical Engineering, University of Bath, Bath, BA2 7AY, UK*

[c] *Institute of Soil and Fertiliser, Guizhou Academy of Agricultural Sciences, Guizhou Guiyang 550006, China*

[d] *Sustainable Energy Systems Engineering Group, School of Engineering, Macquarie University, Sydney, NSW, 2109, Australia*

[*] Corresponding author: luowenhai@cau.edu.cn; Ph: +86 18311430503.

Abstract

We compared the performance of conventional and aquaporin thin-film composite forward osmosis (FO) membranes (denoted as HTI and AQP membrane, respectively) for concentration of digested manure centrate. Results show that the two FO membranes were capable to concentrate digested centrate for resource recovery. During concentration of digested manure centrate, a cohesive fouling layer formed on the HTI membrane surface, resulting in more dramatic flux decline and less fouling reversibility in comparison to the AQP membrane. The two FO membranes exhibited effective and comparable rejection of bulk organic matter, total phosphorus, and heavy metals, leading to their notable enrichment in digested manure centrate. By contrast, ammonium nitrogen (NH_4^+-N) was only retained by approximately 40% using the two FO membranes with a slightly higher retention by the HTI membrane, since it was less negatively charged. As a result, total nitrogen was ineffectively rejected by the two FO membranes. It is noteworthy that the HTI membrane also contributed to higher rejection of most antibiotics than the AQP membrane, possibly due to enhanced retention by the fouling layer and retarded forward diffusion. Results from this study evidence the outperformance of the AQP membrane as a new generation FO membrane over its conventional counterpart with respect to antifouling property, while further improvement in membrane selectivity, particularly of monovalent cations (e.g. NH_4^+-N), is needed to advance FO applications in resource recovery from challenging waste streams.

Keywords: Forward osmosis; thin-film composite membrane; aquaporin membrane; digested manure centrate; antibiotics

1. Introduction

Anaerobic digestion has been widely implemented for livestock waste treatment [1]. By anaerobic digestion, livestock wastes can be effectively converted to valuable products, including biogas and digestate. Biogas, as a source of renewable energy, can be used for heat and electricity production. Digestate, as a high quality organic fertiliser, can be used to compromise the financial and environmental costs associated with the use of mineral fertilisers as well as increase agricultural production [2].

Digestate is commonly separated into a solid and a liquid fraction for effective storage before agricultural application [3]. This is due to the fact that digestate is produced throughout the year while agronomic activities are seasonal. The solid fraction of digestate can be easily handled as organic fertiliser, while the liquid fraction, usually named digested centrate, is a vexing challenge to the sustainable management of livestock farms [4].

Digested centrate is an extremely high strength wastewater and can result in severe environmental pollution without appropriate treatment [5]. In particular, risky contaminants, such as heavy metals and antibiotics, present considerably in digested centrate given their abuse for livestock production, high residuals in livestock wastes, and low removal in subsequent treatment by anaerobic digestion [6]. Digested centrate, on the other hand, contains high contents of nutrients, such as humus, ammonium nitrogen (NH_4^+-N), and trace elements that are readily available for plants and crops, and thus is commonly recognised as a source of liquid fertiliser [7]. Nevertheless, the large volume and unbalanced nutrient contents challenge the profitable use of digested centrate, particularly when its long-distance transportation to other agricultural regions is necessary owing to limited farmlands nearby livestock farms [8, 9].

Membrane technologies have been widely considered to concentrate digested centrate into small volumes to reduce the storage footprint and produce balanced nutrients that can be exported as liquid fertilisers to other agricultural regions [10, 11]. Gong et al. [12] reported that a pilot-scale disk tube-reverse osmosis (DT-RO) system could concentrate digested centrate by 4 times with almost complete retention of total nitrogen

(TN) and total phosphorus (TP). Ruan et al. [13] implemented a hybrid membrane system consisted of microfiltration, ultrafiltration, and RO in sequence for concentration of digested centrate and reported that RO could concentrate digested centrate by 5 times with over 97% removal of total ammonia nitrogen (TAN) and organic matter indicated by the measurement of chemical oxygen demand (COD). Similar results have also been reported by Zhou et al. [14] who applied a dual stage RO process to concentrate digested centrate by 5 times with nutrient and clean water recovery of 98% and 92.5%, respectively. Nevertheless, severe membrane fouling occurred in these studies, although advanced pre-treatment techniques, such as centrifugation, physical filtration, and chemical coagulation, were employed. Indeed, fouling has been recognised as a vexing barrier to the techno-economic development of membrane processes for concentration of digested manure centrate due to its massive contents of suspended particles with varying particle size, organic matter (e.g. humic and protein-like substances), colloidal particles, and inorganic substances [15].

Forward osmosis (FO), an osmotically driven membrane process, has been proposed as a low fouling alternative for the treatment of challenging waste streams, such as raw sewage [16, 17], leachate [18, 19], and digested centrate [20-22]. During FO operation, clean water transports from a feed solution, through a semipermeable membrane, into a draw solution with osmotic pressure deviation between these two solutions as the driving force. FO is born with high selectivity, low fouling propensity, and high fouling reversibility, and small energy consumption when the draw solution is appropriately handled [23]. Wu et al. [24] demonstrated that the cellulose triacetate (CTA) FO membrane could concentrate digested manure centrate to trigger spontaneous and in-situ struvite formation with 0.5 M magnesium chloride as the draw solution to contribute a water flux of 3.12 L/m^{2}h. A higher water flux (5 L/m^{2}h) was observed by Kedwell et al. [25] who used the thin-film composite (TFC) FO membrane for phosphorus recovery from digested manure centrate. Indeed, it has been well documented that the TFC membranes outperform their CTA counterparts in FO applications with respect to water permeability and solute selectivity [26, 27].

Recent advances in membrane development have resulted in the emergence of biomimetic aquaporin membranes as the next generation TFC FO membranes [28-30]. Aquaporins are water-channel proteins in the cell membrane with high water permeation (10^9 water molecules per second for each) and effective solute rejection [31]. Previous studies have demonstrated that aquaporin FO membranes exhibited comparable clean water flux, higher contaminant rejection, and much lower reverse solute flux in comparison with conventional TFC FO membranes [32-34]. Nevertheless, little is known about the discrepancy between conventional and aquaporin FO membranes in wastewater treatment and resource recovery. Furthermore, there remains controversy in literature regarding the performance of aquaporin FO membrane in wastewater treatment, particularly the rejection of nitrogen species. Soler-Cabezas et al. [35] reported that the aquaporin FO membrane enabled 66% rejection of NH_4^+-N in concentration of digested sludge centrate. Luo et al. [34] observed a notable decrease in TN removal when the aquaporin FO membrane was used to extract water from an activated sludge bioreactor, possibly due to its low rejection of nitrate and/or nitrite (NO_x^--N). By contrast, more than 95.5% rejection of TAN was demonstrated by Schneider et al. [22] and Camilleri-Rumbau et al. [35] using the aquaporin FO membrane to concentrate digested manure centrate. Thus, further investigation is needed to verify the performance of aquaporin FO membranes and their advances over conventional generations in waste stream treatment.

This study aims to compare the performance between conventional and aquaporin TFC FO membranes for concentration of digested manure centrate. Nutrient enrichment in digested centrate was determined during FO concentration. Rejections of antibiotics and heavy metals were evaluated and related to key physiochemical properties of these two different FO membranes. Membrane fouling behaviours and reversibility were also examined. Results from this study will provide unique insights to the development of FO membranes for resource recovery from challenging waste streams.

2. Materials and methods

2.1 Digested centrate and membranes

129 Digested centrate was collected from a local, small-scale swine farm (Beijing, China),
130 where a black membrane anaerobic digestion pond was constructed for swine waste
131 treatment. In this farm, swine manure and urine were flushed daily to an underground,
132 water-proof reservoir and then pumped into the anaerobic digestion pond. After
133 digested for approximately 20 days, digestate was pumped out and mechanically
134 extruded into a solid and a liquid fraction for storage until farmland application.
135 Digested centrate used here was obtained by naturally settling the liquid fraction of
136 digestate overnight under laboratory conditions as described below for the
137 concentration experiment. Key physiochemical properties of digested centrate are
138 shown in Table 1.

139 **[Table 1]**

140 A biomimetic, aquaporin membrane provided by Aquaporin A/S (Aquaporin A/S,
141 Copenhagen, Denmark) was used and denoted as the AQP membrane. Briefly, the AQP
142 membrane was made as a TFC membrane by stabilising vesicles with embedded
143 aquaporin proteins in a polyamide layer supported by a porous polysulfone supporting
144 layer [29]. A conventional polyamide TFC membrane from Hydration Technology
145 Innovations (HTI, Albany, OR) was used as the benchmark and denoted as the HTI
146 membrane. The HTI membrane was consisted of a thin selective polyamide active layer
147 on the top of a porous polysulfone supporting layer [26]. The HTI membrane was
148 soaked in 25% isopropanol for 15 min and then thoroughly rinsed with deionised water
149 for 2 min to remove vegetable-based glycerine, which was used to protect the
150 membrane surface in shipping. Key transport and physiochemical characteristics of the
151 conventional and aquaporin TFC membranes are summarized in Table S1,
152 Supplementary Data.

153 **2.2 Forward osmosis system and operation**

154 A bench-scale, closed-loop FO system with a cross-flow membrane cell and two
155 variable speed gear pumps was employed (Fig. S1, Supplementary Data). The
156 membrane cell consisted of two separated acrylic blocks to hold a flat-sheet membrane
157 without any physical support. Each acrylic block was engraved to form a flow channel

of 2 mm deep, 50 mm wide, and 100 mm long. The total effective membrane area was 50 cm^2. Two variable speed gear pumps (Micropump, Vancouver, WA) were used to circulate feed and draw solutions at a cross-flow velocity of 8.3 cm/s, respectively. The draw solution reservoir was placed on a digital balance (Mettler ToledoInc., Hightstown, NJ), which was connected to a computer to automatically record weight changes for calculation of permeate water flux.

The FO system was operated in the osmotic dilution mode with digested centrate and 1 M sodium chloride (NaCl) solution as the feed and draw solution, respectively. The initial volumes of feed and draw solutions were 1 L. The membrane active layer faced the feed solution. Each experiment was concluded when the observed water flux decreased to a negligible level. Aqueous samples (5 mL) were taken at intervals from both feed and draw solutions during FO operation. All experiments were conducted in duplicate with new membrane coupons.

The FO membranes after concentration tests were flushed, and then osmotically backwashed to evaluate membrane fouling reversibility. The cross-flow velocity of feed and draw solutions was doubled (i.e. 16.6 cm/s) to flush the membrane for 30 min. Pure water fluxes of the pristine, fouled, flushed, and then osmotically backwashed FO membranes were measured. The FO system was operated for one hour to obtain the average pure water flux with 1 L deionised water feed and 1 M NaCl draw solution. Pure water flux recovery (η) after membrane cleaning was calculated as [36, 37]:

$$\eta(\%) = \frac{J_c - J_a}{J_b - J_a} \times 100 \qquad (1)$$

where J_b and J_a were the pure water flux before and after concentration of digested centrate, respectively; J_c was the pure water flux after membrane cleaning. The water flux recovery indicates membrane fouling reversibility.

2.3 Analytic methods

2.3.1 Basic water quality parameter

Key water quality parameters of digested centrate and draw solution samples were

measured according to standard methods. Specifically, COD was analysed based on the fast digestion spectrophotometric method with high range COD vials (HACH, USA). TN and TP were determined using the alkaline potassium persulfate digestion-UV spectrophotometric method and the ammonium molybdate spectrophotometric method, respectively. NH_4^+-N was measured by a Flow Injection Analysis system (QuikChem 8500, Lachat, CO). An Orion 4-Star Plus pH/conductivity meter (Thermo Scientific, Waltham, MA) was used to measure the solution pH and electrical conductivity. Total solids (TS) and volatile solids (VS) were determined based on the standard method 2540.

2.3.2 Fluorescence excitation-emission matrix spectroscopy

The fluorescence intensity of feed and draw solutions was analysed using a two-dimensional fluorescence spectrophotometer (Perkin-Elmer LS-55) with excitation wavelengths between 200 and 400 nm and emission wavelengths between 200 and 550 nm (in 10 nm increments). It has been well established that fluorophores in certain areas of optical space in an excitation-emission-intensity matrix (EEM) could qualify the specific fractions of dissolved organic matter [38, 39]. All samples were diluted to the same COD concentration (50 mg/L) for fair comparison of EEM spectra. The fluorescence regional integration (FRI) method was used to further analyse the EEM spectra to identify organic distribution [40].

2.3.3 Heavy metals and antibiotics

Heavy metals and antibiotics in the feed and draw solutions were analysed at the beginning and conclusion of each concentration experiment. The feed and draw solutions were centrifuged at 4000 g for 20 mins to obtain the supernatants for analysis. Key heavy metals, including chromium (Cr), nickel (Ni), arsenic (As), selenium (Se), iron (Fe), copper (Cu), zinc (Zn), manganese (Mn), cadmium (Cd), and lead (Pb), were analysed by an inductively coupled plasma-optical emission spectrometry (710 ICP-OES, Agilent Technologies, CA). Antibiotics belonged to three widely used groups, namely sulfonamides, quinolones, and tetracyclines, were analysed based on the method in previous publications [6, 41]. Briefly, the analytical method included solid

phase extraction (SPE), derivatization, and quantification by an ultrahigh performance liquid chromatography-tandem mass spectrometry (UPLC-MS/MS, Waters, Milford, MA). Ethylenediaminetetraacetic acid disodium salt (EDTA-2Na) was added to the supernatants at a concentration of 1.5 g/L to minimize the influence of metals on antibiotic extraction.

2.3.4 Contaminant rejection calculation

Contaminant rejection by the FO membrane was determined based on the mass balance [42]:

$$R(\%) = \left(1 - \frac{C_{DS(f)} V_{DS(f)} - C_{DS(i)} V_{DS(i)}}{C_{FS(i)} V_{FS(i)}}\right) \times 100 \qquad (2)$$

where $C_{DS(i)}$ and $C_{DS(f)}$ were contaminant concentrations in the draw solution at the beginning and conclusion of each experiment, respectively. Since a clean NaCl solution was used, contaminants were absent from the raw draw solution (i.e. $C_{DS(i)} = 0$). $V_{DS(i)}$ and $V_{DS(f)}$ were the volume of draw solution before and after FO concentration. $C_{FS(i)}$ and $V_{FS(i)}$ were contaminant concentrations in the feed solution and its volume at the beginning of FO operation, respectively.

A mass balance analysis was also conducted by comparing contaminant presence in both feed and draw solutions before and after concentration experiments. This analysis quantifies contaminant escape from the feed and draw solutions, for example, by evaporation, biodegradation, and adsorption onto the membrane, during FO concentration.

2.3.5 Membrane characterization

Membrane autopsy was conducted at the conclusion of each concentration experiment. Membrane surface morphology and composition were characterised by a scanning electron microscopy (SEM) coupled with energy dispersive spectroscopy (EDS) (JCM-6000, JEOL, Tokyo, Japan). Membrane samples were air-dried in a desiccator and then coated with an ultra-thin gold layer with a sputter coater (SPI Module, West Chester, PA). Membrane surface functional groups were identified using an Attenuated Total

241 Reflection-Fourier Transform Infrared (ATR-FTIR) spectroscopy (IRAffinity-1,
242 Shimadzu, Kyoto, Japan). Absorbance spectra were measured with 20 scans at a
243 spectral resolution of 2 cm^{-1} for each membrane sample. A background correction was
244 conducted before each measurement.

245 **3. Results and discussion**

246 *3.1 Water flux and membrane fouling*

247 Water fluxes of two FO membranes decreased continuously during concentration of
248 digested manure centrate (Fig. 1A). The water flux decline could be attributed to
249 membrane fouling, osmotic dilution of the draw solution, and concentration of the feed
250 solution. Either concentrated feed solution or diluted draw solution could reduce the
251 effective osmotic driving force and thus water flux [17]. Compared to the AQP
252 membrane, more considerable decline in water flux was observed for the HTI
253 membrane. This observation was possibly due to higher reverse solute flux and more
254 severe fouling of the HTI membrane in comparison to the AQP membrane. Reverse
255 solute flux, an inherent phenomenon in FO, could augment salinity build-up in the feed
256 solution and reduction in the draw solution. In this study, the reverse solute flux was
257 approximately 14.1 ± 2.1 g/m^2h (calculated as total dissolved solids, TDS) for the HTI
258 membrane, which was much higher than that of the AQP membrane (3.98 ± 0.63 g/m^2h)
259 in concentration of digested manure centrate given its larger salt permeability (Table
260 S1, Supplementary Data). Furthermore, the pure water flux of the HTI membrane
261 decreased by 60.8%, which was approximately 4.5 times higher than the flux reduction
262 of the AQP membrane after concentration of digested manure centrate (Fig. 1B). As a
263 result, the AQP membrane could be operated for nearly 38 hours to recover 67.9% water
264 from digested manure centrate until the water flux decreased to a negligible level in
265 comparison to 62.0% water recovery within 49 hours for the HTI membrane (Fig. S2,
266 Supplementary Data).

267 **[Figure 1]**

268 The AQP membrane exhibited much higher fouling reversibility than the HTI

membrane after concentration of digested manure centrate (Fig. 1B). The pure water flux of the AQP membrane was recovered by 73.9% from 14.9 to 16.6 L/m^{2}h after physical flushing for 30 min. Additional water flux recovery up to 78.3% could be achieved by osmotic backwashing. Chun et al. [30] also reported that physical cleaning largely restored the water flux of the AQP membrane, but could not completely remove foulants scattered on the membrane surface. By contrast, the pure water flux of the HTI membrane was increased from approximately 6.8 to 13.3 L/m^{2}h with a total flux recovery of 60.6% by physical flushing and then osmotic backwashing. As the AQP membrane (-13.6 ± 1.76 mV) was more negatively charged than the HTI membrane (-8.1 ± 1.94 mV) (Table S1, Supplementary Data), its lower fouling propensity and higher fouling reversibility were possibly due to the stronger electrostatic repulsion between membrane surface and organic foulants (i.e. humic- and protein-like substances) [43]. Moreover, the incorporation of globular aquaporin vesicles on the AQP membrane surface [33] could smoothen the surface roughness of the polyamide selective layer to alleviate foulant deposition [23].

After concentration of digested manure centrate, a cohesive fouling layer fully covered on the HTI membrane surface. The SEM-EDS results indicate that the fouling layer was consisted of organic and inorganic foulants (Fig. 2A). Indeed, the ATR-FTIR spectra show that the fouled HTI membrane exhibited distinctive adsorption peaks at 2922 cm^{-1}, which usually associates with alkane (C-H stretching) in aliphatic structures, at 1644 cm^{-1}, suggesting alkene (C=C) in aliphatic structures and/or amide I (C=O) bonds, and at 1575cm^{-1}, representing amide II (C-N-H) bonds, in comparison to the pristine membrane (Fig. 2B). Since small organic matter, such as protein-like substances, could pass through the FO membrane [44], organic foulants were also detected on the supporting layer of the HTI membrane (Fig. S3, Supplementary Data). By contrast, the fouling layer scattered on AQP membrane surface, which was also composed of organic and inorganic substances as indicated by the SEM-EDS and ATR-FTIR measurements (Fig. 2C&D). As discussed above, this observation could be attributed to the low fouling propensity of the AQP membrane and the detachment of loose fouling layer

from the membrane surface during concentration of digested manure centrate. Similar results have also been reported by Soler-Cabezas et al. [21] who observed a decrease and then increase in the AQP membrane water flux during concentration of digested sludge centrate due to fouling layer detachment.

[Figure 2]

3.2 Organic and nutrient enrichment in the feed solution

Both organic matter and nutrients were enriched considerably when the two FO membranes were used to concentrate digested manure centrate (Fig. 3). The COD content in the feed solution was concentrated by approximately 2.8 and 2.3 times for the AQP and HTI membranes, respectively (Fig. 3A), when their water fluxes decreased to a negligible level. The higher COD content encountered by the AQP membrane could be mainly attributed to its higher water recovery (Fig. 1A), since its rejection of organic substances (approximately 75%) was comparable to the HTI membrane (Fig. 4). The EEM spectra and subsequent FRI analysis indicate that tyrosine-like and tryptophan-like proteins as well as small molecular weight soluble microbial byproduct-like substances could pass through the two FO membranes (Fig. S4, Supplementary Data). Thus, by the end of FO concentration, the COD content in the draw solution was 1649.1 ± 74.5 and 1542.4 ± 86.9 mg/L, corresponding to a forward organic flux of 10.3 ± 0.46 and 12.6 ± 0.71 g COD/m^2h for the HTI and AQP membrane, respectively. Such a larger forward organic flux of the AQP membrane could be related to its higher water flux in comparison to the HTI membrane (Fig. 1).

[Figure 3]

The TP content in the feed solution increased similarly for the two FO membranes (Fig. 3B), due to their high and comparable phosphorus rejection (Fig. 4). It has been reported that almost complete rejection of phosphorus ions could be achieved by the FO membrane due to their large hydrated radius and electrostatic repulsion against negatively charged membrane surface [20, 22]. As a result, TP was indiscernible in the draw solution using these two FO membranes to concentrate digested manure centrate.

Compared to the HTI membrane, the AQP membrane could only result in a slightly higher TP concentration in the feed solution due to its higher water recovery when the concentration experiment was concluded.

[Figure 4]

A much lower enrichment by the two FO membranes occurred to nitrogen in comparison to bulk organic matter and phosphorus (Fig. 3). As shown in Fig. 3C, the TN content in digested manure centrate was concentrated by 1.5 times using either AQP or TFC membrane. This result was possibly due to the low rejection of nitrogen species, particularly NH_4^+-N, by the two FO membranes (Fig. 4). It has been well established that TN in digested manure centrate was mainly contributed by NH_4^+-N given the ammonification of organic matter and the absence of nitrification in anaerobic digestion [3, 45]. In this study, NH_4^+-N accounted for more than 50% of TN in raw digested manure centrate (Table 1). In addition, the low TN accumulation could also be attributed to its volatilisation from the feed solution and/or attachment onto the membrane surface during concentration of digested manure centrate, which may be driven by shifting of feed stream pH value. Indeed, a mass balance analysis shows that approximately 6.3% and 3.6% TN escaped from either feed and draw solutions when the HTI and AQP membranes were used, respectively. Similar results have also been reported by Masse et al. [46] and Mondor et al. [47] who demonstrated that over 15% TN volatised during manure concentration by RO at an ambient temperature (21 – 24 ºC).

Despite the concentration of digested centrate, the NH_4^+-N content decreased slightly in the feed solution (Fig. 3D). This decrease could be mainly attributed to the ineffective rejection of NH_4^+-N by the FO membranes (Fig. 4) and its evaporation as NH_3 from the feed solution. The low NH_4^+-N rejection by the FO membranes could be attributed to its small radius (0.104 nm) and electrostatic attraction [48, 49]. Moreover, NH_4^+-N could convert to NH_3, which is more evaporable and permeable through the membrane [25], particularly with an increase in the feed solution pH caused by the diffusion of protons to the draw solution in FO operation [17]. It is noteworthy that the increased alkalinity of the feed solution could also result in the deprotonation of the membrane

355 polyamide layer, augmenting the exchange of monovalent cations between the feed and
356 draw solution [50]. In addition, the decreased NH_4^+-N content in the feed solution could
357 also be ascribed partially to the spontaneous and in-situ struvite precipitation in the feed
358 stream with enhanced concentration of relevant ions [24].

359 The AQP membrane exhibited a lower NH_4^+-N rejection than the HTI membrane (Fig.
360 4). This result was possibly owing to the more negatively charged surface and higher
361 water flux of the AQP membrane in comparison with the HTI membrane (Fig. 1). Lu et
362 al. [51] reported that a more negatively charged membrane surface could dramatically
363 enhance the bidirectional diffusion of cations (i.e. NH_4^+ and Na^+) between the feed and
364 draw solution as driven by Donnan dialysis. Kedwell et al. [25] observed that ammonia
365 loss was exacerbated with an increase in the water flux during FO concentration of
366 digested sludge centrate. In addition, the lower NH_4^+-N rejection of the AQP membrane
367 could also be related to its smaller solute permeability coefficient and thus lower reverse
368 solute flux (Table S1, Supplementary Data). Schneider et al. [22] demonstrated that the
369 reverse diffusion of chloride ions could cause a charge imbalance and thus trigger the
370 transport of anions from the feed solution to the draw solution to restore the charge
371 equilibrium, leading to NH_4^+-N accumulation in the feed solution during FO operation.
372 As a result, the forward NH_4^+-N flux was 3.40 ± 0.21 g/m^{2}h for the AQP membrane,
373 which was much higher than that of the HTI membrane (2.27 ± 0.04 g/m^{2}h), resulting
374 in NH_4^+-N accumulation up to approximately 900 mg/L (nearly 47.5% of TN) in the
375 draw solution by the conclusion of FO concentration.

376 *3.3 Rejection of heavy metals*

377 Six out of ten heavy metals that occur ubiquitously in swine manure were detectable in
378 raw digested centrate (Fig. 5). Of the six heavy metals, Cr, As, and Se exhibited notable
379 residuals, possibly due to their high addition to livestock feedstocks. For instance,
380 organic As compounds has been widely used as feed additives to improve swine health
381 and growth; Cr may present in livestock feed and consequently manure due to the
382 impurity of dicalcium phosphate supplements [52].

383 **[Figure 5]**

All heavy metals measured here accumulated considerably at the conclusion of FO operation (Fig. 5A). Since the two FO membranes exhibited an effective and comparable rejection of all heavy metals (> 80%) (Fig. 5B), their more enrichment in the feed solution for the AQP membrane was driven by its higher water recovery. Similar results have also been reported by Vital et al. [53] in the treatment of acid mine drainage using conventional TFC FO membranes and could be attributed to the large hydrate radius of these heavy metals and their electrostatic repulsion against the negatively charged membrane surface [54].

3.4 Rejection of antibiotics

In this study, 15 compounds belonged to three groups of widely used antibiotics (i.e. sulfonamides, quinolones, and tetracyclines) were detected in raw digested centrate (Fig. 6). Of the three groups of antibiotics, tetracyclines had the highest concentrations, due to their high residuals in livestock excretes and ineffective removal by anaerobic digestion [6, 55]. Since these antibiotics could be retained by the two FO membranes (Fig. 7), their concentrations increased along with the concentration of digested manure centrate (Fig. 6).

[Figure 6]

The rejection of antibiotics by the two FO membranes varied significantly (Fig. 7). Compared to sulfonamides and quinolones, tetracyclines were more effectively rejected, possibly due to their large molecular weight. Pan et al. [56] also reported that tetracyclines could be highly retained (> 97%) by conventional TFC FO membranes in pharmaceutical wastewater treatment. Despite the incorporation of highly selective aquaporin vesicles into the membrane selective layer and the smaller estimated pore radius (Table S1, Supplementary Data), the AQP membrane exhibited a lower rejection of almost all antibiotics in comparison with the HTI membrane. It has been reported that the AQP membrane was more effective than the HTI membrane for the retention of negatively charged and non-ionic hydrophilic micro-pollutants in a clean feed solution consisted of 20 mM NaCl and 1 mM $NaHCO_3$[33]. Thus, the higher removal of antibiotics by the HTI membrane observed in this study was possibly due to their

enhanced retention by the thick fouling layer fully covered on the membrane surface (Fig. 2A). Xie et al. [57] demonstrated that the fouling layer on the FO membrane surface could contribute to pore blockage and thus enhanced steric hindrance to increase the rejection of micro-pollutants, including pharmaceuticals, personal care products, and endocrine disrupters, that occur ubiquitously in municipal wastewater. In addition, reverse draw solute flux could hinder the forward diffusion of feed solutes, through a phenomenon known as 'retarded forward diffusion', thereby reducing their permeation through the FO membrane [58]. As a result, the higher antibiotic rejection observed for the HTI membrane could also result from its larger solute permeability coefficient and thus higher reverse draw solute flux than the AQP membrane (Table S1, Supplementary Data).

[Figure 7]

Although the HTI membrane exhibited better rejection of antibiotics, their concentrations in the feed solution were slightly higher for the AQP membrane at the conclusion of FO operation (Fig. 6). This observation could be ascribed to the slightly higher water recovery contributed by the AQP membrane (Fig. 1) and antibiotic adsorption onto the fouling layer formed on the HTI membrane surface. In addition, the HTI membrane was operated longer to obtain a water recovery comparable to the AQP membrane (section 3.1), and thus, antibiotics were more susceptible to biodegradation. Previous studies have demonstrated the further biodegradation of organic matter for biogas production during storage of digested manure centrate [4, 59]. Furthermore, Li et al. [3] observed a continuous decrease in the concentration of all 17 antibiotics belonged to tetracyclines, quinolones, and sulphonamides in both liquid and solid fractions of manure digestate during storage under different scenarios. Indeed, the digested centrate used in this study was still biologically active as indicated by its VS/TS ratio higher than 0.5 (Table 1). A mass balance analysis also shows the loss of most antibiotics from the bulk feed and draw solutions during FO concentration, particularly when the HTI membrane was used (Fig. S5, Supplementary Data).

4. Environmental implications

High selectivity and low fouling propensity of the FO membrane impart its technological charm to concentrate digested manure centrate for the production of high quality liquid fertiliser. High solute rejection of the FO membrane ensures nutrient enrichment in digested manure centrate, and on the other hand, results in the accumulation of risky contaminants, such as heavy metals and antibiotics. Thus, digested manure centrate should be treated prior to FO concentration, for example, by chemical and electrochemical coagulation-flocculation [60], to reduce contaminant occurrence and simultaneously maintain nutrient contents. Moreover, nutrients and contaminants, mainly small molecular weight organic substances and NH_4^+-N, could permeate through highly selective FO membranes. Hence, apart from the design and fabrication of next-generation FO membranes, additional processes, such as membrane distillation and activated carbon adsorption [39], would be deployed downstream to purify the draw solution for clean water production.

5. Conclusion

Results reported here show that the AQP membrane outperformed partially the HTI membrane during FO concentration of digested manure centrate for resource recovery. Compared to the HTI membrane, the AQP membrane exhibited less fouling propensity and higher fouling reversibility to augment water recovery from digested manure centrate. Nevertheless, the two FO membranes contributed to comparable and effective retention of bulk organic matter, heavy metals, and TP, thereby resulting in their considerable enrichment in the feed solution. Contrarily, the two FO membranes were ineffective to retain nitrogen species, leading to low TN rejection and accumulation in the feed stream. In particular, the rejection of NH_4^+-N by the AQP membrane was much lower than that by the HTI membrane. Moreover, the HTI membrane was more capable to retain antibiotics in comparison to the AQP membrane. However, antibiotic accumulation in digested manure centrate was lower for the HTI membrane by the conclusion of FO concentration.

6. Acknowledgement

This research was supported under the Key Program of the Natural Science Foundation of Guizhou Province, China (Project No. 20191452) and the National Natural Science Foundation of China (Project No. 51708547).

7. Reference

[1] Bolzonella, D., Fatone, F., Gottardo, M., and Frison, N. (2018). Nutrients recovery from anaerobic digestate of agro-waste: Techno-economic assessment of full scale applications. J. Environ. Manage., 216: 111-119.

[2] Mao, C., Feng, Y., Wang, X., and Ren, G. (2015). Review on research achievements of biogas from anaerobic digestion. Renew. Sustain. Energ. Rev., 45: 540-555.

[3] Li, Y., Liu, H., Li, G., Luo, W., and Sun, Y. (2018). Manure digestate storage under different conditions: Chemical characteristics and contaminant residuals. Sci. Total Environ., 639: 19-25.

[4] Gioelli, F., Dinuccio, E., and Balsari, P. (2011). Residual biogas potential from the storage tanks of non-separated digestate and digested liquid fraction. Bioresour. Technol., 102(22): 10248-51.

[5] Sui, Q., Jiang, C., Yu, D., Chen, M., Zhang, J., Wang, Y., and Wei, Y. (2018). Performance of a sequencing-batch membrane bioreactor (SMBR) with an automatic control strategy treating high-strength swine wastewater. J. Hazard. Mater., 342: 210-219.

[6] Liu, H., Pu, C., Yu, X., Sun, Y., and Chen, J. (2018). Removal of tetracyclines, sulfonamides, and quinolones by industrial-scale composting and anaerobic digestion processes. Environ. Sci. Pollut. Res. Int., 25(36): 35835-35844.

[7] Nkoa, R. (2013). Agricultural benefits and environmental risks of soil fertilization with anaerobic digestates: a review. Agron. Sustain. Dev., 34(2): 473-492.

[8] Masse, L., Massé, D.I., and Pellerin, Y. (2007). The use of membranes for the treatment of manure: a critical literature review. Biosyst. Eng., 98(4): 371-380.

[9] Tampio, E., Marttinen, S., and Rintala, J. (2016). Liquid fertilizer products from anaerobic digestion of food waste: mass, nutrient and energy balance of four digestate liquid treatment systems. J. Clean. Prod., 125: 22-32.

[10] Masse, L., Mondor, M., and Dubreuil, J. (2013). Membrane filtration of the liquid fraction from a solid-liquid separator for swine manure using a cationic polymer as flocculating agent. Environ. Technol., 34(5-8): 671-7.

[11] Xie, M., Shon, H.K., Gray, S.R., and Elimelech, M. (2016). Membrane-based processes for wastewater nutrient recovery: Technology, challenges, and future direction. Water Res., 89: 210-21.

[12] Gong, H., Wang, Z., Zhang, X., Jin, Z., Wang, C., Zhang, L., and Wang, K. (2017). Organics and nitrogen recovery from sewage via membrane-based pre-concentration combined with ion exchange process. Chem. Eng. J., 311: 13-19.

[13] Ruan, H., Yang, Z., Lin, J., Shen, J., Ji, J., Gao, C., and Van der Bruggen, B. (2015). Biogas slurry concentration hybrid membrane process: Pilot-testing and RO membrane cleaning. Desalination, 368: 171-180.

[14] Zhou, Z., Chen, L., Wu, Q., Zheng, T., Yuan, H., Peng, N., and He, M. (2019). The

valorization of biogas slurry with a pilot dual stage reverse osmosis membrane process. Chem. Eng. Res. Des., 142: 133-142.
[15] Akhiar, A., Battimelli, A., Torrijos, M., and Carrere, H. (2017). Comprehensive characterization of the liquid fraction of digestates from full-scale anaerobic co-digestion. Waste Manag., 59: 118-128.
[16] Xue, W., Yamamoto, K., and Tobino, T. (2016). Membrane fouling and long-term performance of seawater-driven forward osmosis for enrichment of nutrients in treated municipal wastewater. J. Membr. Sci., 499: 555-562.
[17] Ansari, A.J., Hai, F.I., Guo, W., Ngo, H.H., Price, W.E., and Nghiem, L.D. (2016). Factors governing the pre-concentration of wastewater using forward osmosis for subsequent resource recovery. Sci. Total Environ., 566-567: 559-566.
[18] Dong, Y., Wang, Z., Zhu, C., Wang, Q., Tang, J., and Wu, Z. (2014). A forward osmosis membrane system for the post-treatment of MBR-treated landfill leachate. J. Membr. Sci., 471: 192-200.
[19] Iskander, S.M., Zou, S., Brazil, B., Novak, J.T., and He, Z. (2017). Energy consumption by forward osmosis treatment of landfill leachate for water recovery. Waste Manag., 63: 284-291.
[20] Holloway, R.W., Childress, A.E., Dennett, K.E., and Cath, T.Y. (2007). Forward osmosis for concentration of anaerobic digester centrate. Water Res., 41(17): 4005-14.
[21] Soler-Cabezas, J.L., Mendoza-Roca, J.A., Vincent-Vela, M.C., Luján-Facundo, M.J., and Pastor-Alcañiz, L. (2018). Simultaneous concentration of nutrients from anaerobically digested sludge centrate and pre-treatment of industrial effluents by forward osmosis. Sep. Purif. Technol., 193: 289-296.
[22] Schneider, C., Rajmohan, R.S., Zarebska, A., Tsapekos, P., and Helix-Nielsen, C. (2019). Treating anaerobic effluents using forward osmosis for combined water purification and biogas production. Sci. Total Environ., 647: 1021-1030.
[23] Mi, B. and Elimelech, M. (2010). Organic fouling of forward osmosis membranes: Fouling reversibility and cleaning without chemical reagents. J. Membr. Sci., 348(1-2): 337-345.
[24] Wu, Z., Zou, S., Zhang, B., Wang, L., and He, Z. (2018). Forward osmosis promoted in-situ formation of struvite with simultaneous water recovery from digested swine wastewater. Chem. Eng. J., 342: 274-280.
[25] Kedwell, K.C., Quist-Jensen, C.A., Giannakakis, G., and Christensen, M.L. (2018). Forward osmosis with high-performing TFC membranes for concentration of digester centrate prior to phosphorus recovery. Sep. Purif. Technol., 197: 449-456.
[26] Cath, T.Y., Elimelech, M., McCutcheon, J.R., McGinnis, R.L., Achilli, A., Anastasio, D., Brady, A.R., Childress, A.E., Farr, I.V., Hancock, N.T., Lampi, J., Nghiem, L.D., Xie, M., and Yip, N.Y. (2013). Standard methodology for evaluating membrane performance in osmotically driven membrane processes. Desalination, 312: 31-38.
[27] Zhang, B., Song, X., Nghiem, L.D., Li, G., and Luo, W. (2017). Osmotic membrane bioreactors for wastewater reuse: Performance comparison between cellulose

556 triacetate and polyamide thin film composite membranes. J. Membr. Sci., 539:
557 383-391.
558 [28] Tang, C., Wang, Z., Petrinić, I., Fane, A.G., and Hélix-Nielsen, C. (2015).
559 Biomimetic aquaporin membranes coming of age. Desalination, 368: 89-105.
560 [29] Zhao, Y., Vararattanavech, A., Li, X., Helixnielsen, C., Vissing, T., Torres, J., Wang,
561 R., Fane, A.G., and Tang, C.Y. (2013). Effects of proteoliposome composition
562 and draw solution types on separation performance of aquaporin-based
563 proteoliposomes: implications for seawater desalination using aquaporin-based
564 biomimetic membranes. Environ. Sci. Technol., 47(3): 1496-503.
565 [30] Chun, Y., Qing, L., Sun, G., Bilad, M.R., Fane, A.G., and Chong, T.H. (2018).
566 Prototype aquaporin-based forward osmosis membrane: Filtration properties
567 and fouling resistance. Desalination, 445: 75-84.
568 [31] Jensen, M.O. and Mouritsen, O.G. (2006). Single-channel water permeabilities of
569 Escherichia coli aquaporins AqpZ and GlpF. Biophys. J., 90(7): 2270-84.
570 [32] Madsen, H.T., Bajraktari, N., Hélix-Nielsen, C., Van der Bruggen, B., and Søgaard,
571 E.G. (2015). Use of biomimetic forward osmosis membrane for trace organics
572 removal. J. Membr. Sci., 476: 469-474.
573 [33] Xie, M., Luo, W., Guo, H., Nghiem, L.D., Tang, C.Y., and Gray, S.R. (2018). Trace
574 organic contaminant rejection by aquaporin forward osmosis membrane:
575 Transport mechanisms and membrane stability. Water Res., 132: 90-98.
576 [34] Luo, W., Xie, M., Song, X., Guo, W., Ngo, H.H., Zhou, J.L., and Nghiem, L.D.
577 (2018). Biomimetic aquaporin membranes for osmotic membrane bioreactors:
578 Membrane performance and contaminant removal. Bioresour. Technol., 249:
579 62-68.
580 [35] Camilleri-Rumbau, M.S., Soler-Cabezas, J.L., Christensen, K.V., Norddahl, B.,
581 Mendoza-Roca, J.A., and Vincent-Vela, M.C. (2019). Application of aquaporin-
582 based forward osmosis membranes for processing of digestate liquid fractions.
583 Chem. Eng. J., 371: 583-592.
584 [36] Xie, M., Lee, J., Nghiem, L.D., and Elimelech, M. (2015). Role of pressure in
585 organic fouling in forward osmosis and reverse osmosis. J. Membr. Sci., 493:
586 748-754.
587 [37] Mo, Y., Tiraferri, A., Yip, N.Y., Adout, A., Huang, X., and Elimelech, M. (2012).
588 Improved antifouling properties of polyamide nanofiltration membranes by
589 reducing the density of surface carboxyl groups. Environ. Sci. Technol., 46(24):
590 13253-61.
591 [38] Henderson, R.K., Baker, A., Murphy, K.R., Hambly, A., Stuetz, R.M., and Khan,
592 S.J. (2009). Fluorescence as a potential monitoring tool for recycled water
593 systems: a review. Water Res., 43(4): 863-81.
594 [39] Xie, M. and Gray, S.R. (2016). Transport and accumulation of organic matter in
595 forward osmosis-reverse osmosis hybrid system: Mechanism and implications.
596 Sep. Purif. Technol., 167: 6-16.
597 [40] Chen, W., Westerhoff, P., Leenheer, J.A., and Booksh, K. (2003). Fluorescence
598 Excitation−Emission Matrix Regional Integration to Quantify Spectra for
599 Dissolved Organic Matter. Environ. Sci. Technol., 37: 5701-5710.

600 [41] Luo, W., Phan, H.V., Xie, M., Hai, F.I., Price, W.E., Elimelech, M., and Nghiem,
601 L.D. (2017). Osmotic versus conventional membrane bioreactors integrated
602 with reverse osmosis for water reuse: Biological stability, membrane fouling,
603 and contaminant removal. Water Res., 109: 122-134.
604 [42] Xie, M., Nghiem, L.D., Price, W.E., and Elimelech, M. (2014). Relating rejection
605 of trace organic contaminants to membrane properties in forward osmosis:
606 measurements, modelling and implications. Water Res., 49: 265-74.
607 [43] Mazlan, N.M., Marchetti, P., Maples, H.A., Gu, B., Karan, S., Bismarck, A., and
608 Livingston, A.G. (2016). Organic fouling behaviour of structurally and
609 chemically different forward osmosis membranes – A study of cellulose
610 triacetate and thin film composite membranes. J. Membr. Sci., 520: 247-261.
611 [44] Luo, W., Arhatari, B., Gray, S.R., and Xie, M. (2018). Seeing is believing: Insights
612 from synchrotron infrared mapping for membrane fouling in osmotic membrane
613 bioreactors. Water Res., 137: 355-361.
614 [45] Ledda, C., Schievano, A., Salati, S., and Adani, F. (2013). Nitrogen and water
615 recovery from animal slurries by a new integrated ultrafiltration, reverse
616 osmosis and cold stripping process: a case study. Water Res., 47(16): 6157-66.
617 [46] Masse, L., Masse, D., and Pellerin, Y. (2008). The effect of pH on the separation
618 of manure nutrients with reverse osmosis membranes. J. Membr. Sci., 325(2):
619 914-919.
620 [47] Mondor, M., Masse, L., Ippersiel, D., Lamarche, F., and Masse, D.I. (2008). Use
621 of electrodialysis and reverse osmosis for the recovery and concentration of
622 ammonia from swine manure. Bioresour. Technol., 99(15): 7363-8.
623 [48] Valladares Linares, R., Li, Z., Abu-Ghdaib, M., Wei, C.-H., Amy, G., and
624 Vrouwenvelder, J.S. (2013). Water harvesting from municipal wastewater via
625 osmotic gradient: An evaluation of process performance. J. Membr. Sci., 447:
626 50-56.
627 [49] Xue, W., Tobino, T., Nakajima, F., and Yamamoto, K. (2015). Seawater-driven
628 forward osmosis for enriching nitrogen and phosphorous in treated municipal
629 wastewater: effect of membrane properties and feed solution chemistry. Water
630 Res., 69: 120-130.
631 [50] Arena, J.T., Chwatko, M., Robillard, H.A., and McCutcheon, J.R. (2015). pH
632 Sensitivity of Ion Exchange through a Thin Film Composite Membrane in
633 Forward Osmosis. Environ. Sci. Technol. Lett., 2(7): 177-182.
634 [51] Lu, X., Boo, C., Ma, J., and Elimelech, M. (2014). Bidirectional diffusion of
635 ammonium and sodium cations in forward osmosis: role of membrane active
636 layer surface chemistry and charge. Environ. Sci. Technol., 48(24): 14369-76.
637 [52] Wang, H., Dong, Y., Yang, Y., Toor, G.S., and Zhang, X. (2013). Changes in heavy
638 metal contents in animal feeds and manures in an intensive animal production
639 region of China. J. Environ. Sci., 25(12): 2435-2442.
640 [53] Vital, B., Bartacek, J., Ortega-Bravo, J.C., and Jeison, D. (2018). Treatment of acid
641 mine drainage by forward osmosis: Heavy metal rejection and reverse flux of
642 draw solution constituents. Chem. Eng. J., 332: 85-91.
643 [54] Qiu, M. and He, C. (2019). Efficient removal of heavy metal ions by forward

osmosis membrane with a polydopamine modified zeolitic imidazolate framework incorporated selective layer. J. Hazard. Mater., 367: 339-347.
[55] Wallace, J.S., Garner, E., Pruden, A., and Aga, D.S. (2018). Occurrence and transformation of veterinary antibiotics and antibiotic resistance genes in dairy manure treated by advanced anaerobic digestion and conventional treatment methods. Environ. Pollut., 236: 764-772.
[56] Pan, S.-F., Zhu, M.-P., Chen, J.P., Yuan, Z.-H., Zhong, L.-B., and Zheng, Y.-M. (2015). Separation of tetracycline from wastewater using forward osmosis process with thin film composite membrane – Implications for antibiotics recovery. Sep. Purif. Technol., 153: 76-83.
[57] Xie, M., Nghiem, L.D., Price, W.E., and Elimelech, M. (2014). Impact of organic and colloidal fouling on trace organic contaminant rejection by forward osmosis: Role of initial permeate flux. Desalination, 336: 146-152.
[58] Xie, M., Nghiem, L.D., Price, W.E., and Elimelech, M. (2012). Comparison of the removal of hydrophobic trace organic contaminants by forward osmosis and reverse osmosis. Water Res., 46(8): 2683-2692.
[59] Balsari, P., Dinuccio, E., and Gioelli, F. (2013). A floating coverage system for digestate liquid fraction storage. Bioresour. Technol., 134: 285-289.
[60] Luo, H., Lyu, T., Muhmood, A., Xue, Y., Wu, H., Meers, E., Dong, R., and Wu, S. (2018). Effect of flocculation pre-treatment on membrane nutrient recovery of digested chicken slurry: Mitigating suspended solids and retaining nutrients. Chem. Eng. J., 352: 855-862.

667 **LIST OF FIGURES**

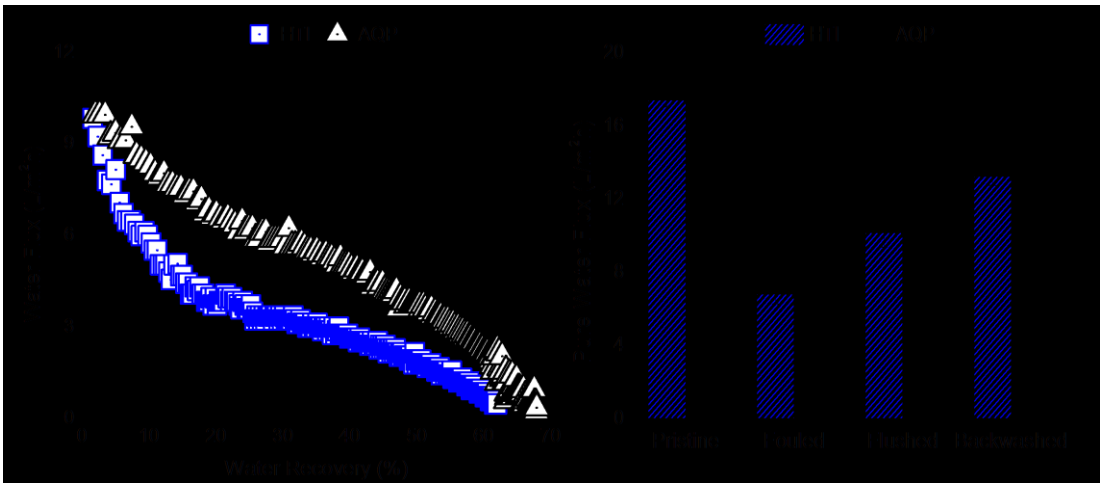

668

669 **Fig. 1:** Water fluxes of the HTI and AQP FO membranes (A) and their fouling
670 reversibility (B) during concentration of digested manure centrate. The FO process was
671 operated in the osmotic dilution mode with 1 L digested centrate and 1 L NaCl solution
672 (1 M) as the initial feed and draw solutions at a cross-flow velocity of 8.3 cm/s,
673 respectively. Error bar represents standard deviation from duplicate experiments.

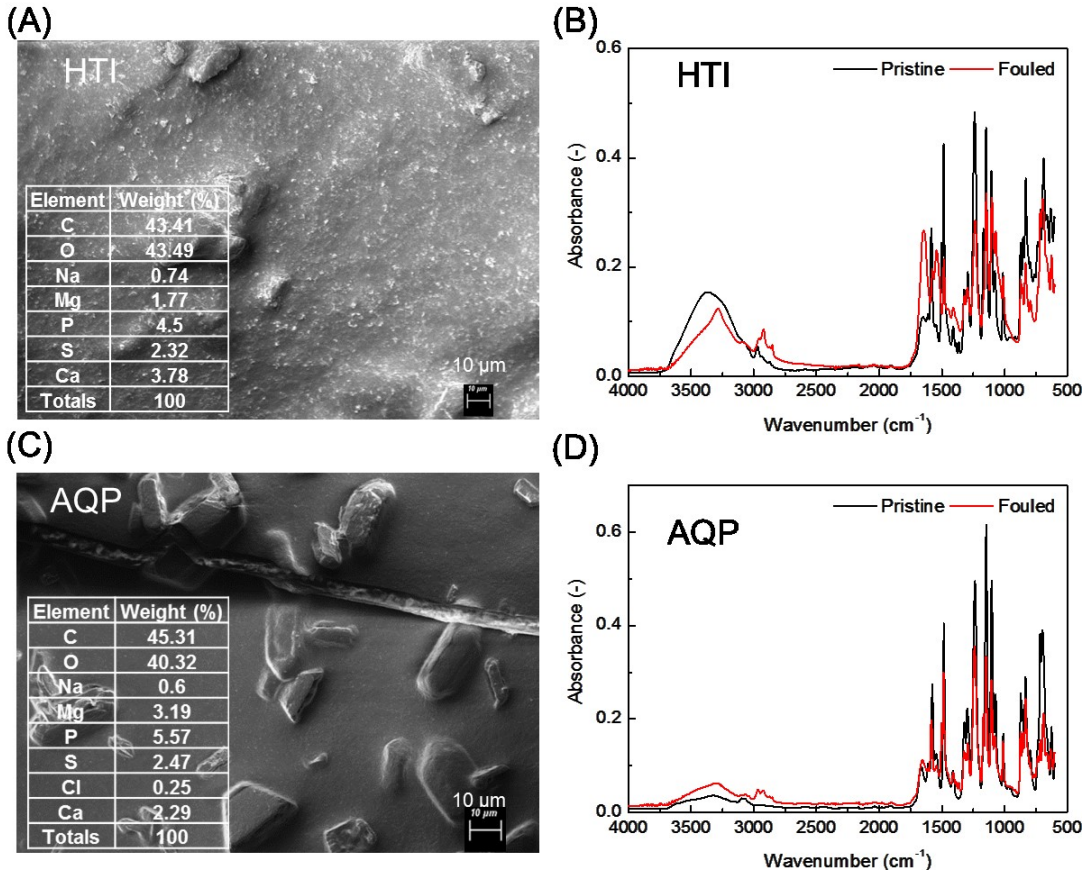

674

675 **Fig. 2:** SEM and EDS measurements of the active layer of (A) HTI and (B) AQP
676 membranes after concentrating digested manure centrate. Results from the EDS
677 measurement were inserted inside the SEM images to show the elementary
678 compositions of the fouling layer. Experimental conditions are as shown in the caption
679 of Fig. 1.

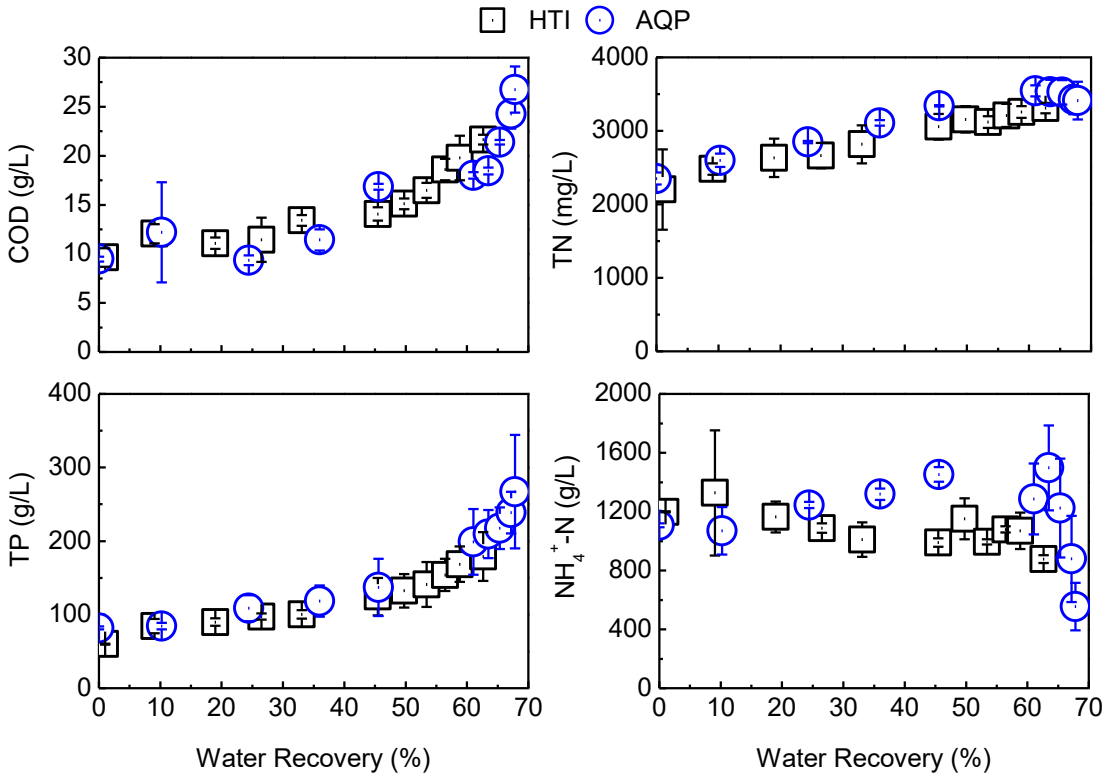

680

681 **Fig. 3:** Enrichment of bulk organic matter and nutrients in the feed solution during
682 concentration of digested manure centrate by the HTI and AQP FO membranes.
683 Experimental conditions are given in the caption of Fig. 1. Error bar represents standard
684 deviation from duplicate experiments.

685

686

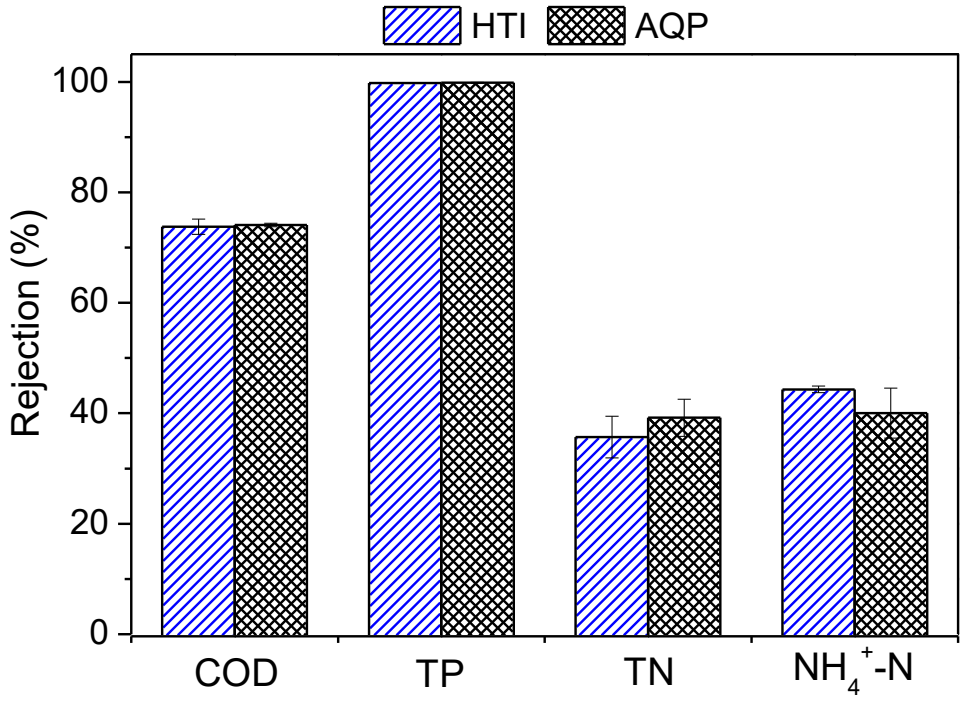

687

688 **Fig. 4:** Rejection of bulk organic matter and nutrients by the HTI and AQP FO
689 membranes during concentration of digested manure centrate. Experimental conditions
690 are as described in the caption of Fig. 1. Error bar represents standard deviation from
691 duplicate experiments.

692

693

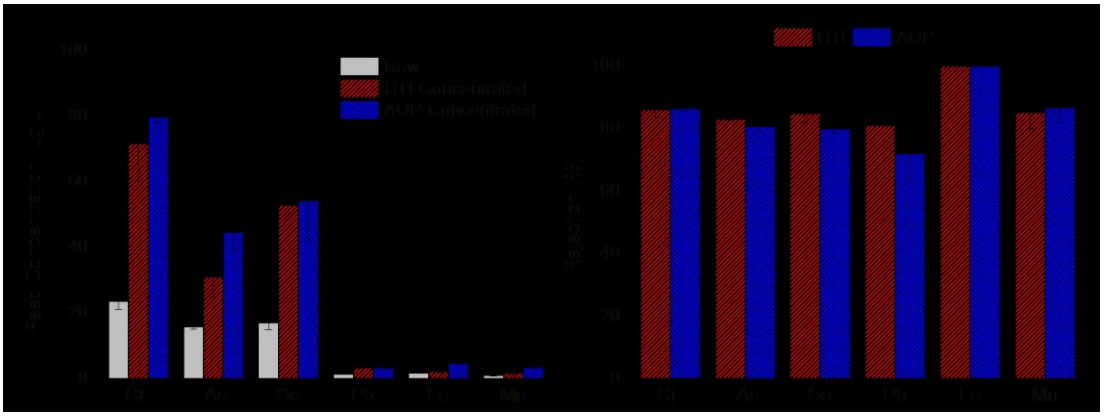

694

695 **Fig. 5:** Enrichment of heavy metals in the feed solution (A) and their rejection by the
696 HTI and AQP FO membranes (B) during concentration of digested manure centrate.
697 Experimental conditions are given in the caption of Fig. 1. Error bar represents standard
698 deviation from duplicate experiments.

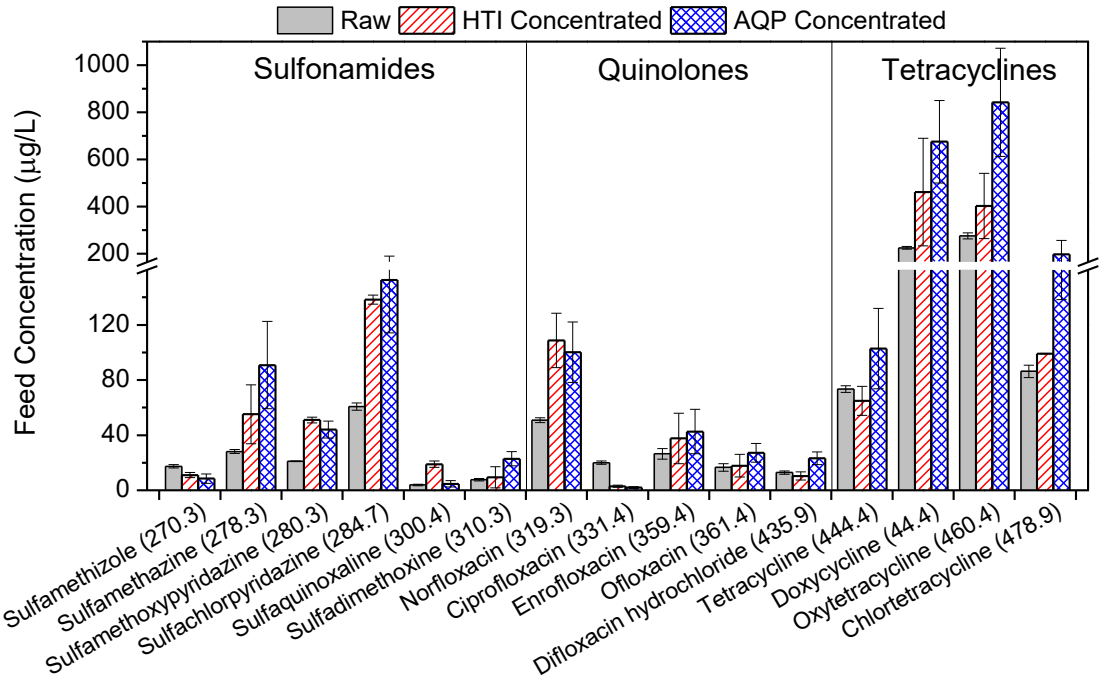

699

700 **Fig. 6:** Antibiotic concentrations in the feed solution during concentration of digested
701 manure centrate by the HTI and AQP FO membranes. Antibiotics were ordered based
702 on their molecular weights shown in the parentheses. Experimental conditions are given
703 in the caption of Fig. 1. Error bar represents standard deviation from duplicate
704 experiments.

705

706

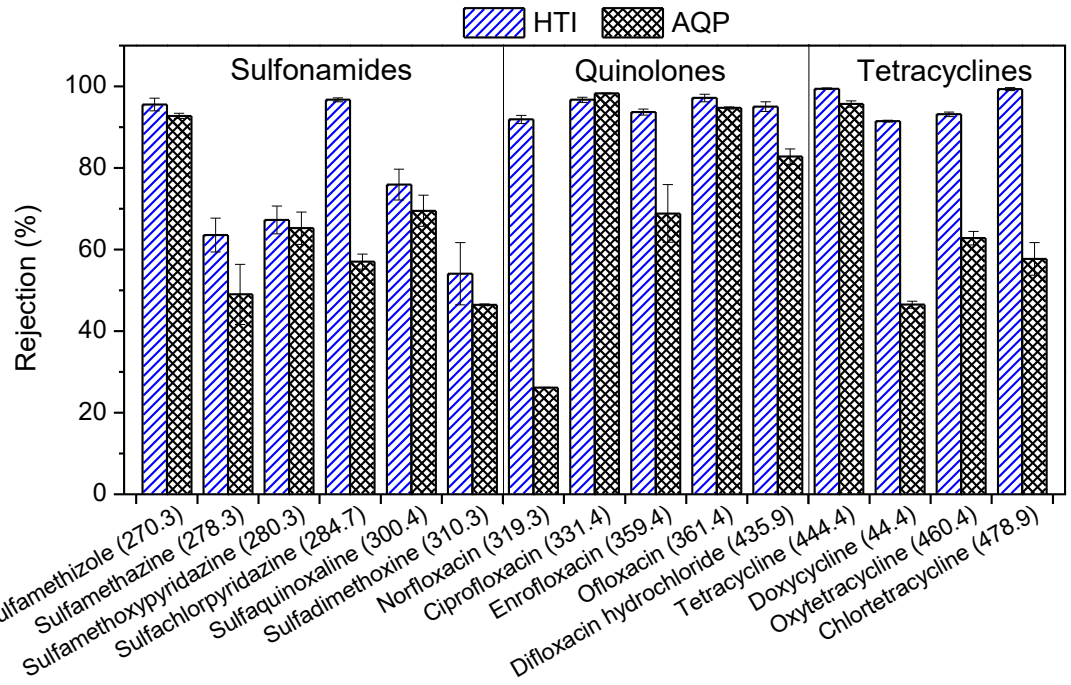

707

708 **Fig. 7:** Rejection of antibiotics by the HTI and AQP FO membranes during
709 concentration of digested manure centrate. Experimental conditions are given in the
710 caption of Fig. 1. Error bar represents standard deviation from duplicate experiments.

LIST OF TABLES

Table 1: Key physiochemical characteristics of digested manure centrate used in this study (mean values ± standard deviation from duplicate experiments)

Chemical oxygen demand, COD (mg/L)	9550 ± 569
Total nitrogen, TN (mg/L)	2276 ± 330
Total phosphorus, TP (mg/L)	70.9 ± 12.8
Ammonium nitrogen, NH_4^+-N (mg/L)	1152 ± 53.5
pH (-)	7.2 ± 0.1
Electrical conductivity (mS/cm)	10.3 ± 1.2
Total solids, TS (mg/L)	9077 ± 88
Volatile solids, VS (mg/L)	6075 ± 297
VS/TS (-)	0.67 ± 0.04